Earthquake detection capability of the Swiss Seismic Network

K.Z. Nanjo[1], D. Schorlemmer[2], J. Woessner[3], S. Wiemer[3], D. Giardini[3]

[1]University of Tokyo; [2]University of Southern California; [3]Swiss Seismological Service, ETH Zürich, E-mail: kazuyoshinanjo@yahoo.co.jp

Abstract

A reliable estimate of completeness magnitudes is vital for many seismicity- and hazard-related studies. Here we adopted and further developed the new Probability-based Magnitude of Completeness (PMC) method (Schorlemmer & Woessner 2008). This method determines network detection completeness (M_P) using only empirical data: earthquake catalog, phase picks, and station information. To evaluate the applicability to low- or moderate-seismicity regions, we performed a case study in Switzerland. The Swiss Seismic Network (SSN) at present is recording seismicity with one of the densest networks of broad-band sensors in Europe. Based on data from 1 January 1983 to 31 March 2008, we found strong spatio-temporal variability of network completeness: the highest value of M_P in Switzerland at present is 2.5 in the Geneva area, close to the national boundary, while M_P is lower than 1.6 in high-seismicity areas (Graubünden, Valais, and Aargau). Thus, events of magnitude 2.5 can be detected at the probability level 0.9999 in all of Switzerland.

Furthermore, we

1) investigated the temporal evolution of M_P for the last 20 years, showing the improvement of the SSN.

2) introduced the calculation of uncertainties to the probabilistic method using a bootstrap approach resulting in uncertainties in completeness magnitudes generally less than 0.1 magnitude units.

3) explored the possible use of PMC as a network planning tool with simulating installations of one or more virtual stations to assess the completeness and identify appropriate locations for new station installations.

We compared our results with an existing study of the completeness based on detecting the point of deviation from a power-law in the earthquake-size distribution. In general, the new approach provides higher estimates than the traditional one. We associate this observation with the difference in the sensitivity of the two approaches in periods where the event detectability of the seismic networks is low. Our results allow us to move towards a full description of completeness as a function of space and time, which can be used for hazard-model development and forecast-model testing, showing an illustrative example of the applicability of the PMC method to regions with low to moderate seismicity.

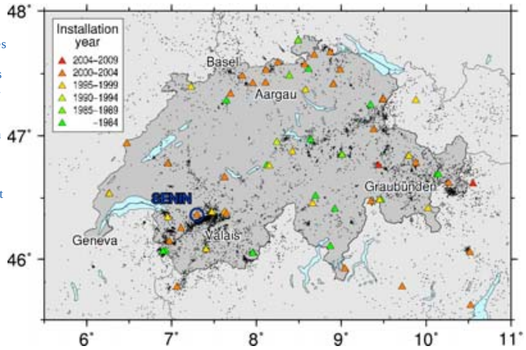

Fig. 1. Location map of seismograph stations (triangles) and earthquakes (circles) in and around Switzerland. Station colors indicate installation times. Station "SENIN" is highlighted; a broadband 3-component seismograph in operation since 26 February 2002 at the location of 7.299° E and 46.363° N, and the height of 2035 m. Swiss borders are shown in thick solid curves. Geographical references are included.

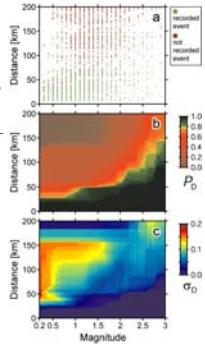

Fig. 2. Detection characteristic of station "SENIN", highlighted in Fig. 1. (a) Distribution of 1890 not picked (red) and 1958 picked (green) events for the station. (b) Detection-probability distribution, P_D. (c) Distribution of uncertainties of P_D, σ_D.

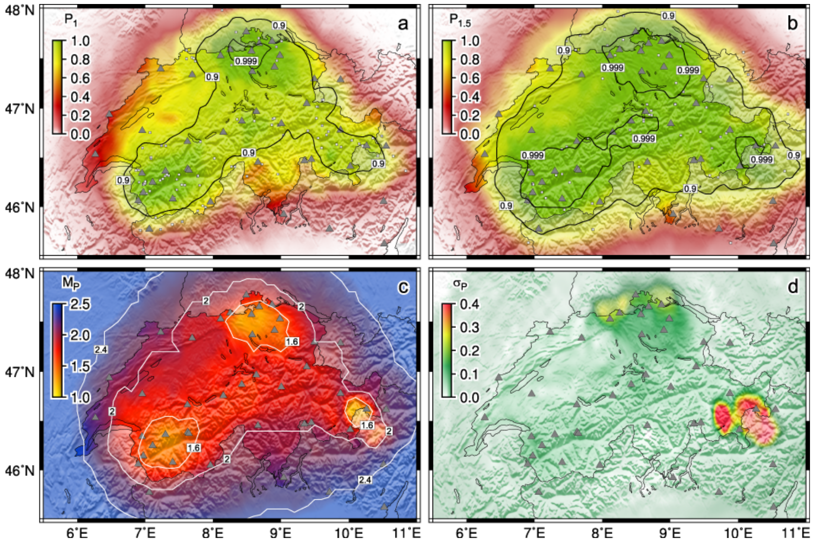

Fig. 3. Maps of network detection probabilities (a) $P1 = P_E|M = 1$ and (b) $P1.5 = P_E|M = 1.5$ for the stations (marked as triangles) in operation on 1 April 2008. Gray circles mark earthquakes of respective magnitude that were recorded in the previous two years. Black lines show contours of $P_E = 0.9$ and $P_E = 0.999$. (c) Map of probability-based completeness, M_P, for the same day and set of stations. White lines show contours for $M_P = 1.6$, $M_P = 2.0$, and $M_P = 2.4$. (d) Map of uncertainties of M_P, σ_P.

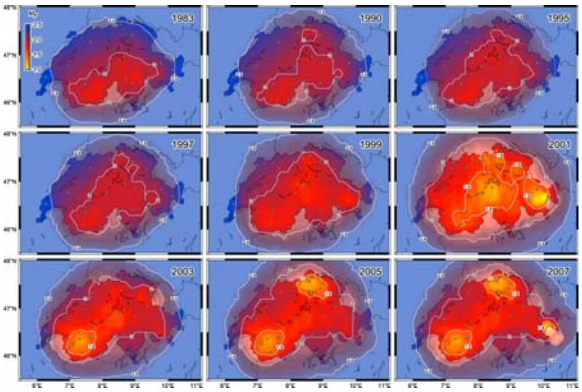

Fig. 4. Maps of probability-based magnitude of completeness, M_P, for different points in times. All maps show M_P at 1 January of the respective year as indicated in the frames (1983, 1990, 1995, 1997, 1999, 2001, 2003, 2005, and 2007). White lines show contours for $M_P = 1.6$, $M_P = 2.0$, and $M_P = 2.4$.

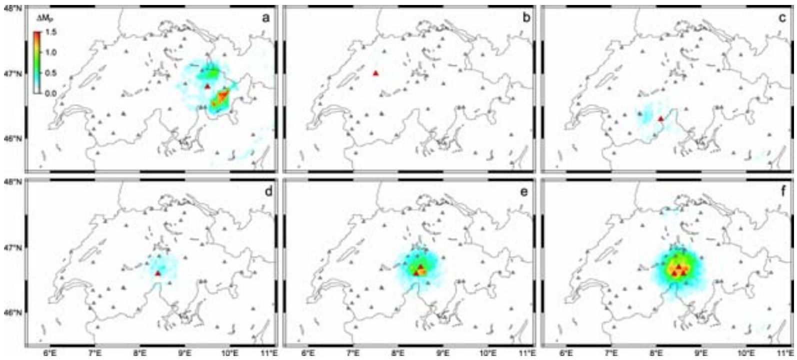

Fig. 5. Scenario computations of adding virtual stations to the network to examine their effect on network detection capabilities. Virtual stations were added to the SSN in operation on 1 April 2008. The station locations are (a) 9.5° E/46.8° N, (b) 7.5° E/47.0° N, (c) 8.1° E/46.3° N, (d) 8.4° E/46.6° N. (e) We added another station (8.5° E/46.7° N) to this configuration. (f) We added a third station (8.6° E/46.6° N). Color coded is the difference in completeness magnitude between virtual case (M_{PV}) and real case (M_P) in Fig. 3. The detection-probability distribution, P_D, for each virtual station is the same as that for the closest real station.

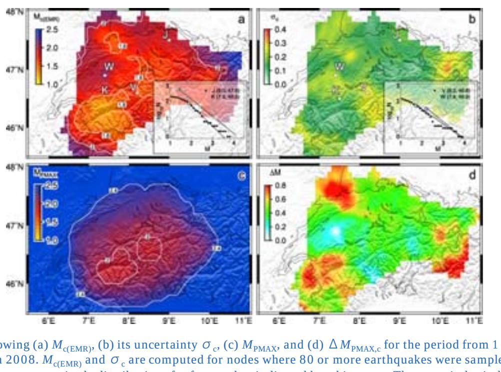

Fig. 6. Maps showing (a) $M_{c(EMR)}$, (b) its uncertainty σ_c, (c) M_{PMAX}, and (d) $\Delta M_{PMAX,c}$ for the period from 1 January 1983 to 31 March 2008. $M_{c(EMR)}$ and σ_c are computed for nodes where 80 or more earthquakes were sampled. The insets show frequency-magnitude distributions for four nodes, indicated by white stars. The gray circles indicate the completeness magnitude, $M_{c(EMR)}$, of each distribution.

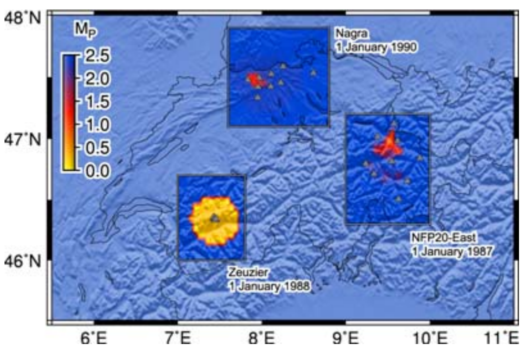

Fig. 7. Map of probability-based magnitude of completeness, M_P, for temporary networks: Nagra network on 1 January 1990, NFP20-East network on 1 January 1987, and Zeuzier network on 1 January 1988. In each frame, the stations of the respective network are shown as triangles. Note that the color scale used here is different from that used in the other figures.